Clinical Science (2015) **128**, 735–747 (Printed in Great Britain) doi: 10.1042/CS20140445

commentary

Original Paper

Exacerbation of acute kidney injury by bone marrow stromal cells from rats with persistent renin–angiotensin system activation

Esko Kankuri*, Elina E. Mervaala*, Markus Storvik†, Aija M.J. Ahola*, Jouko Levijoki‡, Dominik N. Müller§, Piet Finckenberg* and Eero M. Mervaala*

*Faculty of Medicine, Department of Pharmacology, University of Helsinki, Finland
†School of Pharmacy, University of Eastern Finland, Kuopio, Finland
‡Orion Pharma Research Center, Espoo, Finland
§Max Delbrück Center, Experimental and Clinical Research Center, Berlin, Germany

Abstract

Hypertension and persistent activation of the renin–angiotensin system (RAS) are predisposing factors for the development of acute kidney injury (AKI). Although bone-marrow-derived stromal cells (BMSCs) have shown therapeutic promise in treatment of AKI, the impact of pathological RAS on BMSC functionality has remained unresolved. RAS and its local components in the bone marrow are involved in several key steps of cell maturation processes. This may also render the BMSC population vulnerable to alterations even in the early phases of RAS pathology. We isolated transgenic BMSCs (TG-BMSCs) from young end-organ-disease-free rats with increased RAS activation [human angiotensinogen/renin double transgenic rats (dTGRs)] that eventually develop hypertension and die of end-organ damage and kidney failure at 8 weeks of age. Control cells (SD-BMSCs) were isolated from wild-type Sprague–Dawley rats. Cell phenotype, mitochondrial reactive oxygen species (ROS) production and respiration were assessed, and gene expression profiling was carried out using microarrays. Cells' therapeutic efficacy was evaluated in a rat model of acute ischaemia/reperfusion-induced AKI. Serum urea and creatinine were measured at 24 h and 48 h. Acute tubular damage was scored and immunohistochemistry was used for evaluation for markers of inflammation [monocyte chemoattractant protein (MCP-1), ED-1], and kidney injury [kidney injury molecule-1 (KIM-1), neutrophil gelatinase-associated lipocalin (NGAL)]. TG-BMSCs showed distinct mitochondrial morphology, decreased cell respiration and increased production of ROS. Gene expression profiling revealed a pronounced pro-inflammatory phenotype. In contrast with the therapeutic effect of SD-BMSCs, administration of TG-BMSCs in the AKI model resulted in exacerbation of kidney injury and high mortality. Our results demonstrate that early persistent RAS activation can dramatically compromise therapeutic potential of BMSCs by causing a shift into a pro-inflammatory phenotype with mitochondrial dysfunction.

Key words: acute kidney injury, bone marrow, renin–angiotensin system.

INTRODUCTION

Components of the renin–angiotensin system (RAS) form the major basis for the homoeostatic control of blood pressure and sodium balance. Overt or persistent pathological activation of RAS has been tightly linked with hypertension and end-organ damage [1,2]. In addition to the classical endocrine RAS system, several tissue-specific RAS have been described [3]. The local RAS in cells of the bone marrow (BM-RAS) was described a decade ago [4,5] and it has been shown to contribute to several steps during the regulation of cell differentiation during haemopoiesis and erythropoiesis [6]. Inhibition of RAS of bone-marrow-derived stromal cells (BMSCs), for example, has been shown to improve their therapeutic efficacy in a model of myocardial infarction [7]. Although pathologies causing dysfunction of BM-RAS have been implicated in atherosclerosis and haematological malignancies

Abbreviations: AKI, acute kidney injury; AngII, angiotensin II; AT_1 receptor, angiotensin II type 1 receptor; AT_2 receptor, angiotensin II type 2 receptor; ATN, acute tubular necrosis; BM-RAS, RAS in cells of the bone marrow; BMSC, bone-marrow-derived stromal cell; dTGR, double transgenic rat; FCCP, carbonyl cyanide *p*-trifluoromethoxyphenylhydrazone; KIM-1, kidney injury molecule-1; MCP-1, monocyte chemoattractant protein 1; MMP, matrix metalloproteinase; NGAL, neutrophil gelatinase-associated lipocalin; OCR, oxygen consumption rate; qPCR, quantitative real-time PCR; RAS, renin–angiotensin system; ROS, reactive oxygen species; S-, serum; SD, Sprague–Dawley; SLPI, secretory leucocyte protease inhibitor; SOD, superoxide dismutase; TG-BMSC, transgenic BMSC; TGF-β, transforming growth factor-β; WST1, water-soluble tetrazolium salt 1.

Correspondence: Professor Eero Mervaala (email eero.mervaala@helsinki.fi).

via abnormalities in bone-marrow-derived progenitors [5,8,9], less is known about how early subclinical but yet persistent RAS pathology that eventually progresses to end-organ damage could affect the function of bone marrow progenitors. As BMSCs are released from the bone marrow upon tissue injury, and they contribute to several aspects of tissue repair, the tissue-damaging effects of abnormal RAS, or even BM-RAS, could be mediated by and manifested in these cells.

Acute kidney injury (AKI) denotes an abrupt loss of kidney function. One frequent cause of AKI is renal ischaemia [10,11], prompted by a sudden reduction of renal perfusion, leading to cellular injury and tissue destruction. Decreased effective blood flow to the kidneys due to, for example, congestive heart failure or hypertension greatly predisposes the patient to AKI [12]. AKI is associated with very high mortality, and there are currently no effective therapies. Increasing evidence suggests, however, that administration of BMSCs can aid in restoration of kidney function after AKI [13]. BMSCs have been shown to mainly exert their action by homing to the site of injury and stimulating tissue recovery by paracrine inhibition of further inflammatory damage and stimulation of endogenous repair [14]. Interestingly, however, there may be tissue differences in the regenerative response to cell therapy. Recently it was shown that $CD133^+$ chord blood stem cells exacerbate ischaemic AKI, although they exert therapeutic effects in other tissues [15]. This discrepancy further suggests that, although BMSCs show therapeutic effects in general, little is known about how the cells' background and disease-caused alterations affect their regenerative potential.

The double transgenic rat (dTGR) model has been extensively characterized and is widely used for dissecting both blood-pressure-dependent and -independent effects of RAS [3,16–19]. The dTGRs harbour human angiotensinogen and human renin genes, and thus enable evaluation of persistently active RAS in a humanized model system [17,18]. Although the dTGRs eventually develop severe hypertension and die from renal and cardiac end-organ damage at week 8 to 12 [1,16–20], they provide an invaluable and highly reproducible model for studying the pathological contribution of RAS activation on the local tissue level at an early age.

In the present study our aim was to investigate how the early subclinical changes in persistent RAS activation are reflected and conveyed in BMSCs. We especially focused on the therapeutic potential of BMSCs on kidney injury, because persistent RAS activation is associated with end-organ, such as kidney, damage. We harvested BMSCs from dTGRs at 5 weeks of age, i.e. before the animals had developed end-organ damage [19,21], as well as from background-matched normal healthy animals to serve as controls. Cells were transplanted in a model of ischaemia/reperfusion-induced AKI, and their effects were followed for 48 h.

MATERIALS AND METHODS

BMSC isolation and cultures

Five-week-old double transgenic rats harbouring the human angiotensinogen and human renin genes in a Sprague–Dawley (SD) background [18–20] and SD rats from Charles River Laboratories Research Models and Services were used for the studies. After rats were anaesthetized and killed, femoral bones were collected. The ends of the bones were cut, and their bone marrow shafts were flushed with Dulbecco's modified Eagle's medium (DMEM; Life Technologies) containing 5% FBS (Gibco) and antibiotics (Gibco) using a syringe and a 25-30 gauge needle. A total of 2×10 ml of perfusate was collected in sterile tubes, and was then gently pipetted on top of Ficoll Paque Plus (GE Healthcare Europe). After centrifugation the mononuclear fraction was collected, washed with mesenchymal stem cell expansion medium (SCM015, Merck Millipore) containing antibiotics (Gibco), and plated on cell culture dishes. After 1 day, medium was replaced, and adherent cells were cultured to subconfluency, passaged, and used for experiments at passages 5–7.

Mitochondrial staining and MitoSOX measurements

MitoTracker Red (Life Technologies/Molecular Probes) was used for quantification and morphological evaluation of mitochondria. Briefly, 10 000 cells were plated on to a coverslip and were cultured to subconfluency. Slides were incubated with MitoTracker (200 nM) for 1 h and washed with PBS. Fluorescence (λ_{ex} 531 nm/λ_{em} 590 nm) was imaged using Zeiss Axiovert (Carl Zeiss Microimaging). For fluorometric quantification 10 000 cells/well were plated on a 96-well plate. Cells were grown to subconfluency, incubated with MitoTracker as detailed above, washed with PBS, and imaged after addition of 70 μl of expansion medium. A fluorimeter (Wallac Victor, PerkinElmer) at λ_{ex} 531 nm/λ_{em} 590 nm was used for quantification of the emitted fluorescence. Signal intensity was adjusted to amount of protein in each well. Briefly, after fluorescence reading, wells were washed carefully twice with PBS, and 100 μl of RIPA buffer was added to each well. Cells were lysed on ice for 5 min, collected and centrifuged at 8000 ***g*** for 10 min. Protein concentrations were evaluated using the BCA assay (Pierce BCA Protein Assay Kit, ThermoFisher Scientific).

Mitochondrial activity was evaluted using the water-soluble tetrazolium salt 1 (WST-1) cell proliferation reagent (Roche). Similar to the mitochondrial quantification, 10 000 cells/well were grown to subconfluency on a 96-well plate. Fresh expansion medium (100 μl) was replaced at the beginning of the assay, and 10 μl of WST-1 solution was added to each well. The plate was incubated in a cell culture incubator for 2 h, and the absorbance at 450 nm of each well was measured on a plate reader using a reference wavelength of 620 nm (MultiSkan RC, ThermoFisher Scientific). After reading, the cells in each well were lysed and the amount of protein in each well was evaluated as detailed above.

For the evaluation of superoxide production from mitochondria, we used the MitoSox Red probe (Life Technologies/Molecular Probes). Cells (10 000 per well) were grown to subconfluency on a 96-well plate. MitoSox was dissolved in expansion medium, and at the beginning of the experiment the medium was replaced with 200 μl of MitoSOX (5 μM)-containing medium. Cells were incubated in a cell culture incubator for 20 min, and were washed using Hanks balanced salt solution (HBSS; Gibco, Invitrogen). Fluorescence images were taken on

an inverted fluorescence microscope (Olympus IX81) and were analysed using ImageJ 1.46 software (http://rsb.info.nih.gov/ij/).

High-resolution respirometry

Oxygen consumption of BMSC samples was measured with a respirometer (Oxygraph-2k; Oroboros Instruments). Chamber calibration and background calibration were performed as described by the manufacturer (http://oroboros.at, MiPNet protocols 14.06 and 12.06). Air calibrations were done daily. BMSC suspensions in expansion medium were added to the chambers (1×10^6 cells/ml, total volume 2 ml), and spontaneous physiological respiration was evaluated at the routine state. Oligomycin (Sigma–Aldrich) at a final concentration of 5 μM was added to inhibit the ATP synthase. The capacity of the electron transport system was then measured by addition of the uncoupling agent carbonyl cyanide *p*-trifluoromethoxyphenylhydrazone (FCCP; Sigma–Aldrich, 4 μl of 1 mM stock, final concentration 2 μM). Administration of the 4 μl FCCP bolus was repeated until maximal O_2 flux was reached. At the end of the experiment, rotenone (Sigma–Aldrich, final concentration 2.5 μM) was added to estimate the residual O_2 consumption.

Transgenic BMSC (TG-BMSC) mitochondrial respiration

Detailed analysis of the effect of angiotensin II (AngII) and the contribution to AngII autocrine signalling by angiotensin type 1 (AT_1) and AT_2 receptors was carried out using an XFe96 mitochondrial metabolism analyser (Seahorse Bioscience) and the XF Cell Mito Stress Test kit according to the manufacturer's instructions and as outlined previously [22]. Briefly, 1×10^5 TG-BMSCs per well were plated on the XF96 Cell Culture Microplates (Seahorse Bioscience) as indicated with or without the compounds. The compounds used were losartan (10 μM, AT_1 receptor-specific blocker), PD123319 (10 μM, AT_2 receptor-specific blocker) and AngII (100 nM). After an overnight incubation, culture medium was changed to assay medium (Seahorse Bioscience) and the cells were incubated for 1 h before the measurements for oxygen consumption rates (OCRs).

RNA isolation, RT–PCR and microarrays

RNA was isolated from BMSCs (150 000 cells/well) grown to subconfluency on a six-well plate. Cells in each well were lysed with 1 ml of TRIzol® (Molecular Research Center) followed by chloroform/propan-2-ol RNA isolation procedure. RNA concentrations were measured on a Nanodrop 8000 spectrophotometer (Thermo Scientific). All RNA samples were treated with DNase (Sigma, AMPD1-1KT) to remove remnant DNA. cDNA synthesis was carried out from 1 μg of RNA with ImpRomII™ Reverse Transcription System (A3800, Promega), and PCR was performed on a LightCycler 2.0 (Roche) using LightCycler Fast-Start DNA Master SYBR GreenI (Roche). The primers (Sigma–Aldrich) were as follows: rat neutrophil gelatinase-associated lipocalin (NGAL) forward 5′-ACGTCACTTCCATCCTCG-3′; reverse 5′-AGTGTCGGCCACTTGC-3′, human angiotensinogen forward 5′-CGGACAAATCAGCGATG-3′; reverse 5′-GTAGTCCCGCGCTAAA-3′, human renin forward 5′-GCGCGGACTATGTATTTCAGG-3′; reverse 5′-TGCGGTTGTTACGCCGA-3′. Microarrays were performed at Biomedicum Functional Genomics Unit Core Facility (http://www.helsinki.fi/fugu) using Agilent SurePrint GE 8×60k (Agilent Technologies) rat gene expression chips. Microarray data was deposited into the Gene Expression Omnibus (GSE51593) and can be retrieved through the following link http://www.ncbi.nlm.nih.gov/geo/query/acc.cgi?token=qbktkiworlsbxit&acc=GSE51593.

Experimental animals, renal ischaemia/reperfusion, cell therapies and sample preparation

A total of 38 6- to 7-week-old male SD rats were purchased from Charles River Laboratories Research Models and Services. The protocols were approved by the Animal Experimentation Committee of the University of Helsinki, Finland, and the Provincial State Office of Southern Finland (approval number STH059A), whose standards correspond to those of the American Physiological Society. Rats were kept under 12-h light/12-h dark cycle and they had free access to food and water. After a 1 week adaptation period, the rats were divided into five groups: (i) sham-operated controls receiving vehicle (5 ml of 0.9% NaCl/kg intravenous, $n = 6$); (ii) ischaemia/reperfusion group receiving vehicle ($n = 8$); (iii) ischaemia/reperfusion group treated with BMSCs derived from SD rats (2×10^6 cells) ($n = 6$); (iv) ischaemia/reperfusion group with BMSCs derived from SD rats (6×10^6 cells) ($n = 6$); (v) ischaemia/reperfusion group with BMSCs derived from dTGR (2×10^6 cells) ($n = 6$); (vi) ischaemia/reperfusion group with BMSCs derived from dTGR (6×10^6 cells) ($n = 6$). Cell therapies were given intravenously to the carotid artery in the beginning of the reperfusion period, the others received the same volume of vehicle.

An established model of renal ischaemia/reperfusion injury was used [23,24]. Rats were anaesthetized with isoflurane (anaesthesia induction in a chamber with 4–5% isoflurane at a flow rate of 1.5 litres/min), intubated, and 1.5% isoflurane at 1.5 litres/min was used to maintain anaesthesia. Abdominal incisions were made and the renal pedicles were bluntly dissected. Bilateral renal ischaemia was induced by clamping the renal pedicles for 40 min using microvascular clamps. Control animals were subjected to sham operation without renal pedicle clamping. The rats were hydrated with warm saline during the operation and the body temperature was maintained constantly at 37 °C by using a heating pad until awake. The wounds were sutured after removing the clips, and the animals were allowed to recover. Buprenorphine (0.1 mg/kg subcutaneously) was used as post-operative analgesia. At 24 or 48 h after the operation, the rats were anaesthetized with isoflurane, and blood samples were collected from the inferior vena cava with a 5 ml syringe and 22 gauge needle for biochemical measurements. The kidneys were excised, washed with ice-cold saline, blotted dry and weighed. The left kidney was used for Western blot and histological examinations. Tissue samples for histology were fixed in 10% formalin and processed to paraffin with routine methodology. Samples for immunohistochemistry were snap-frozen in −38 °C 2-methylbutane. For protein and gene expression studies, renal samples were snap-frozen in liquid nitrogen. Samples were stored at −80 °C until assayed.

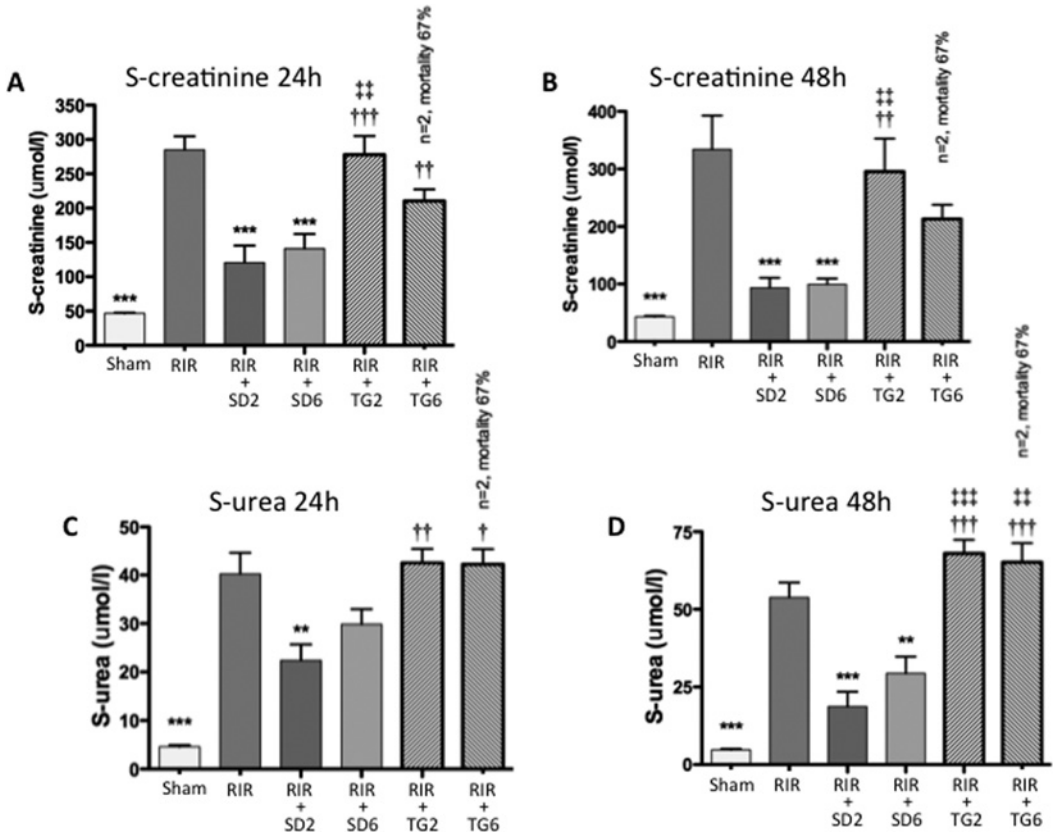

Figure 1 Serum levels of creatinine and urea

Serum creatinine (**A** and **B**) and urea (**C** and **D**) levels at 24- and 48-h time-points after kidney ischaemia/reperfusion injury and indicated treatments. RIR, renal ischaemia/reperfusion; SD2 and SD6, dose of 2 and 6×10^6 SD-BMSCs; TG2 and TG6, dose of 2 and 6×10^6 TG-BMSCs. *Indicates comparison with RIR-group. †Indicates comparison with respective RIR+SD-group. $^{\dagger}P < 0.05$; $^{**,\dagger\dagger}P < 0.01$, $^{***,\dagger\dagger\dagger}P < 0.001$ between groups.

Kidney histology

For histological examination, 4 μm thick paraffin sections were cut and stained with haematoxylin/eosin. Renal samples were visually examined by a pathologist (P.F.) with a Leica DMR microscope, and morphological changes from the whole cross-sectional area of cortex and medulla were assessed according to the acute tubular necrosis (ATN)-scoring system [24] (magnification $\times200$, $\geqslant20$ fields per kidney section quantified using the ATN-scoring system). Evaluation of histopathological changes included the loss of tubular brush border, tubular dilatation, cast formation and cell lysis. Tissue damage was quantified in a blinded manner and scored according to the percentage of damaged tubules in the sample: 0, no damage; 1, less than 25 damage; 2, 25–50 % damage; 3, 50–75 % damage; and 4, more than 75 % damage.

Immunohistochemistry

For immunohistochemistry, frozen kidneys were processed and semi-quantitative scoring of inflammatory cells was performed ($n = 9$–10) as described in detail elsewhere [24]. The relative amount of antibody-positive signal in cortical and medullary areas per sample was determined with computerized densitometry (Leica IM500 and Leica QWIN software). Primary monoclonal antibody against rat monocyte/macrophage ED-1 (Serotec) and peroxidase-conjugated rabbit anti-mouse secondary antibody (Dako) was used.

Biochemical determinations

Serum (S-) creatinine, electrolytes, lipids and liver enzymes were measured by routine laboratory techniques (ADVIA 1650 Chemistry System, Siemens Healthcare Diagnostics).

Statistical analysis

Data are presented as means+S.E.M. Statistically significant differences in mean values were tested by ANOVA and Bonferroni's post-hoc test. The differences were considered significant when $P < 0.05$.

RESULTS

Acute kidney injury

BMSCs from dTG rats (TG-BMSCs) and normal SD control animals (SD-BMSCs) demonstrated a normal stretched-out phenotype characteristic of stromal cells; however, the TG-BMSCs were distinctly smaller. After induction of AKI by

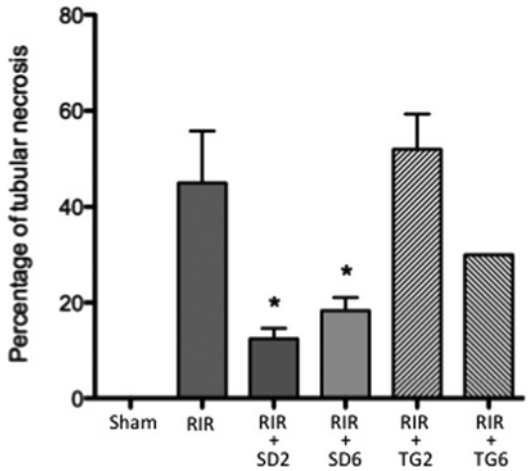

Figure 2 Percentage of tubular necrosis in each group at 48 h from ischaemia/reperfusion injury evaluated from haematoxylin/eosin-stained sections

RIR, renal ischaemia/reperfusion; SD2 and SD6, dose of 2 and 6×10^6 SD-BMSCs; TG2 and TG6, dose of 2 and 6×10^6 TG-BMSCs. $^*P < 0.05$ as compared with the RIR-group.

ischaemia/reperfusion, cells were administered to the abdominal aorta at two concentrations: 2×10^6 and 6×10^6 per animal. As expected, AKI-induced dramatic increases in S-creatinine and S-urea concentrations at both 24 and 48 h time-points were alleviated by administration of SD-BMSCs over time (Figure 1). We observed no significant differences in therapeutic functional response between the different doses (2×10^6 and 6×10^6 cells). Both the SD-BMSCs and the smaller dose of TG-BMSCs were well tolerated by recipients. However, administration of TG-BMSCs demonstrated no therapeutic effects on renal function, as measured by S-creatinine and S-urea. Moreover, after administration of the larger dose of TG-BMSCs, four out of six rats died, further suggesting an overt exacerbation of injury in response to these cells. Owing to this high mortality in the group receiving 6×10^6 TG-BMSCs, no results or statistics can be provided for this group, and the group's results are representative of the two individuals surviving the 2-day follow-up.

The BMSC effect on AKI-induced necrosis was evaluated as the percentage of necrosis from paraffin-embedded tissue sections. Again, the therapeutic effect of SD cells was evident, and in accordance with the functional parameters demonstrating a similar effect for both administered doses (Figure 2). In contrast with SD-BMSCs, however, TG-BMSCs failed to inhibit tubular necrosis and demonstrated no tissue restorative activity.

As BMSCs have been appraised for their anti-inflammatory as well as immunomodulatory activities, we evaluated the amount of activated macrophages (ED-1) and monocyte infiltration [monocyte chemoattractant protein (MCP-1)] 48 h after AKI. Interestingly, administration of both SD- and TG-BMSCs were able to dose-dependently suppress MCP-1 expression, and the TG-BMSCs demonstrated a significantly greater reduction on the amount of activated macrophages (ED-1) that was seen by treatment with SD-BMSCs (Figure 3). We also assessed the renal expression levels of NGAL [25] and kidney injury molecule-1 (KIM-1) [26] as markers of kidney injury (Figure 4). By these parameters, the SD-BMSCs' effect was non-significant as compared with the untreated AKI group, whereas treatment with TG-BMSCs increased both NGAL and KIM-1 expression in the kidneys. Treatment with TG-BMSCs markedly accentuated NGAL expression.

Cellular differences in culture

Compared with the SD-BMSCs, the TG-BMSCs proliferated vigorously with a population doubling time of 77.2 ± 6.2 h compared with 49.2 ± 2.8 h respectively. On the basis of previous results demonstrating disturbances in mitochondrial morphology in cells of dTGR rats [27], we stained mitochondria from both BMSC types using MitoTracker. MitoTracker-emitted fluorescence intensity, indicating the number of mitochondria, was higher from the TG-BMSCs than from a same amount of SD cells (Figures 5A and 5B). Differences in response to cell culture were also evident between SD- and TG-BMSCs. We observed a differential progression of mitochondrial staining intensity between SD- and TG-BMSCs under cell culture conditions over time, and we found the staining intensity of SD-BMSCs to increase over time in comparison with that of TG-BMSCs remaining rather constant. TG-BMSCs' mitochondria were metabolically highly active (WST-1) (Figure 5C) and produced increased amounts of reactive oxygen species (ROS), approximately 3-fold as measured using MitoSOX probe-emitted signal intensity, when compared with the SD control cells (Figure 5D).

Mitochondrial respiration of BMSCs

We then measured the basal oxygen consumption of both TG- and SD-BMSCs. Given the higher rate of cellular proliferation and mitochondrial activity of the TG-BMSCs compared with the SD-BMSC controls, it was surprising to find that the TG-BMSCs consumed significantly less oxygen than the SD control cells (Figure 6). The TG-BMSCs also displayed a greatly diminished maximally stimulated oxygen flux, suggesting disturbances in their mitochondrial electron transport chain. In order to elucidate the functional role of AngII receptor subtypes as well as AngII in the TG-BMSCs, we utilized a mitochondrial respiration measurement system specifically dedicated for cultured cells. After a 24-h incubation with specific receptor blockers for AT_1 and AT_2 (losartan and PD123319 respectively) as well as with AngII, measurement of mitochondrial respiration was carried out. Blocking of either AT_1 or AT_2 receptor subtypes resulted in reduction of baseline OCR and FCCP-stimulated respiration suggesting that receptor stimulation occurs in these cells in an autocrine manner and that both receptor subtypes mediate a similar type of response in terms of mitochondrial respiration (Figure 7). Exogenously added AngII effectively reduced the baseline rate of oxygen consumption as well as the FCCP-stimulated mitochondrial respiration as compared with untreated TG-BMSCs. The effect of exogenous AngII on FCCP-stimulated OCR was also significantly inhibited when compared with either losartan- or PD123319-treated cells.

Gene expression profiling

Although normally the majority of intracellular ROS are produced as a by-product of active mitochondrial respiration [28,29],

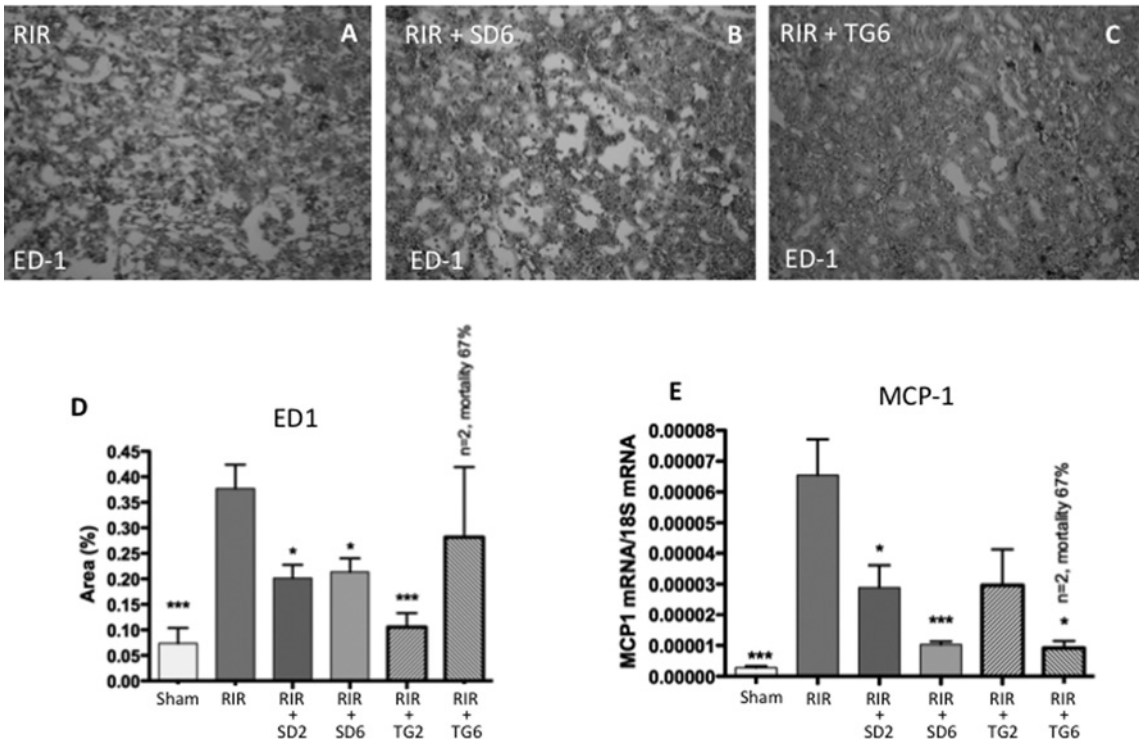

Figure 3 **Renal expression of ED-1 and MCP-1**
Immunohistochemical (IHC) staining (**A**–**C**) for ED-1 to show monocyte and macrophage activation in indicated groups at 48 h after ischaemia/reperfusion injury. RIR, renal ischaemia/reperfusion; SD2 and SD6, dose of 2 and 6×10^6 SD-BMSCs; TG2 and TG6, dose of 2 and 6×10^6 TG-BMSCs. (**D**) Quantification of ED-1-stained area in IHC sections from each group. (**E**) qPCR evaluation of kidney expression of MCP-1 as marker of monocyte chemotaxis at 48 h after ischaemia/reperfusion in indicated groups. $^*P < 0.05$; $^{***}P < 0.001$ as compared with the RIR-group.

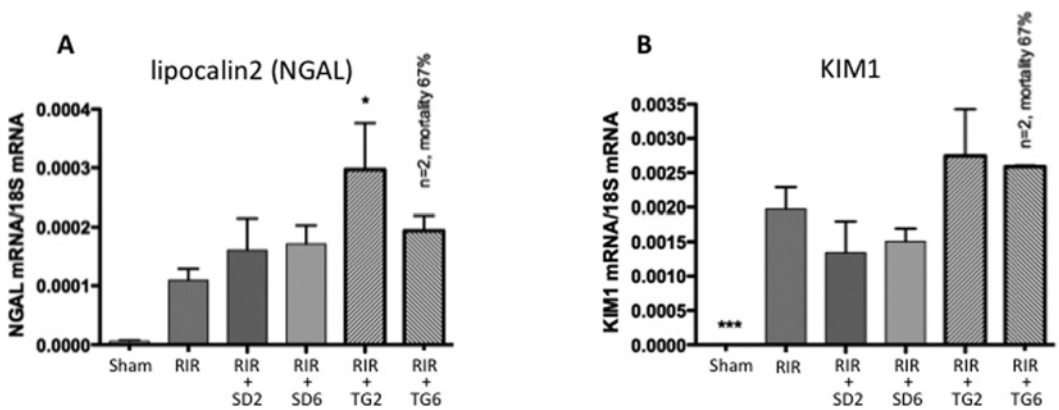

Figure 4 **Renal expression of lipocalin 2 (NGAL) and KIM1**
Evaluation of (**A**) lipocalin 2 (NGAL) and (**B**) KIM1 expression in the kidney by quantitative PCR at 48 h after ischaemia/reperfusion injury. RIR, renal ischaemia/reperfusion; SD2 and SD6, dose of 2 and 6×10^6 SD-BMSCs; TG2 and TG6, dose of 2 and 6×10^6 TG-BMSCs. $^*P < 0.05$; $^{***}P < 0.001$ as compared with the RIR-group.

their production in the TG-BMSCs may be caused by altered mitochondrial oxidative phosphorylation and electron transport putatively also indicating a shift in ATP production towards glycolysis. Moreover, intracellular ROS have been implicated as important players in intracellular signalling and especially in driving processes related to inflammation and aging [29–31]. It could thus be speculated that the TG-BMSCs favour inflammatory signalling. As such a shift, and yet a high proliferation rate, should by definition be characterized by alterations in inflammatory gene expression, we performed whole genome Agilent microarrays to elucidate the effects of BMSC RAS modulation on the cells' gene expression profile. The gene expression changes are shown in Supplementary Tables SI and SII. The KEGG pathways associated with the gene expression changes are shown in Table 1. In TG-BMSCs we observed an over 1000-fold induction in five genes, an over 100-fold induction in 17 genes, and an over

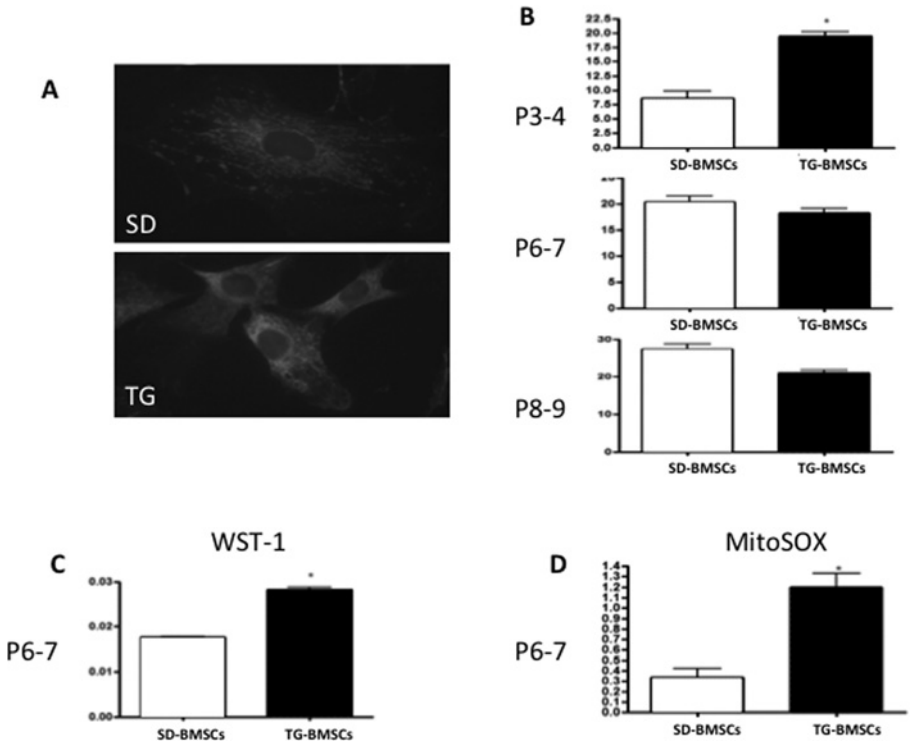

Figure 5 Mitochondrial differences in SD- and TG-BMSCs
(**A**) Mitochondrial staining and morphology by MitoTracker. (**B**) Quantification of MitoTracker mitochondrial staining at the indicated passages (P). (**C**) Evaluation of WST-1 staining as a marker of mitochondrial activity. (**D**) Amount of MitoSOX staining evaluated as a marker for mitochondrial generation of reactive oxygen species. $^{*}P < 0.05$ between cell types.

10-fold induction in a total of 134 genes. The greatest induction of over 2800-fold was seen in the lipocalin 2 (NGAL) gene. Overall, TG-BMSC association with a pro-inflammatory phenotype was evident from these data. Analysis of the endogenous RAS components (Table 2) demonstrated a clear increase in AT_1 receptor expression. Increased expression levels of AT_1 (average 109-fold increase when normalized to 18S expression; average $C_{T\,SD} = 37.3$ compared with $C_{T\,dTGR} = 29.8$), AT_2 (average 2-fold increase when normalized to 18S expression; average $C_{T\,SD} = 36.5$ compared with $C_{T\,dTGR} = 35.1$) and angiotensin-converting enzyme (average 5-fold increase when normalized with 18S expression; average $C_{T\,SD} = 38.9$ compared with $C_{T\,dTGR} = 38.1$) were verified by quantitative real-time PCR (qPCR). The expression of NGAL is shown in Figure 8(A), and demonstrates a more than 10 000-fold increase by qPCR as compared with SD-BMSCs. Although expression of human angiotensinogen was also high (Figure 8B), we did not detect expression of human renin in these cells.

Our data demonstrate that alterations in systemic RAS may manifest in BMSCs and may thus severely compromise these cells' therapeutic efficacy. Overtly active RAS and BM-RAS are characterized by a pro-inflammatory phenotype in BMSCs as shown by high expression of proteolytic enzymes, growth factors and cytokines in this study. Furthermore, alterations in BM-RAS can influence stromal cell proliferation, adherence and lifespan.

DISCUSSION

Both systemic and local bone marrow RAS have been shown to intimately regulate several key steps in maintenance, maturation and differentiation of bone marrow precursors [5,9]. However, only little is known about the functional contribution of persistent RAS activation to the therapeutic potential of BMSCs. In the present study we demonstrated a dramatic exacerbation of ischaemia/reperfusion-induced AKI by transplantation of BMSCs that were isolated from young rats harbouring the human renin and angiotensinogen genes before AngII-induced disease manifestations. Administration of BMSCs isolated from wild-type genetic background controls demonstrated a good therapeutic response. Basal oxygen consumption of the TG-BMSCs was low and the cells' oxidative phosphorylation capacity was decreased. The cells produced increased amounts of mitochondrial ROS. Using gene expression microarrays, we demonstrated massive inductions in expression of inflammation-associated genes such as NGAL, matrix metalloproteinases (MMPs), cytokines and growth factors in TG-BMSCs.

Recently, chronically elevated levels of AngII, as seen in hypertension, have been shown to enhance differentiation of inflammatory cells in the bone marrow utilizing brain-bone marrow sympathetic neuronal circuitry and associated with increased mitochondrial ROS production [32,33]. In concert with these data, our results show that alterations in the host's RAS result early

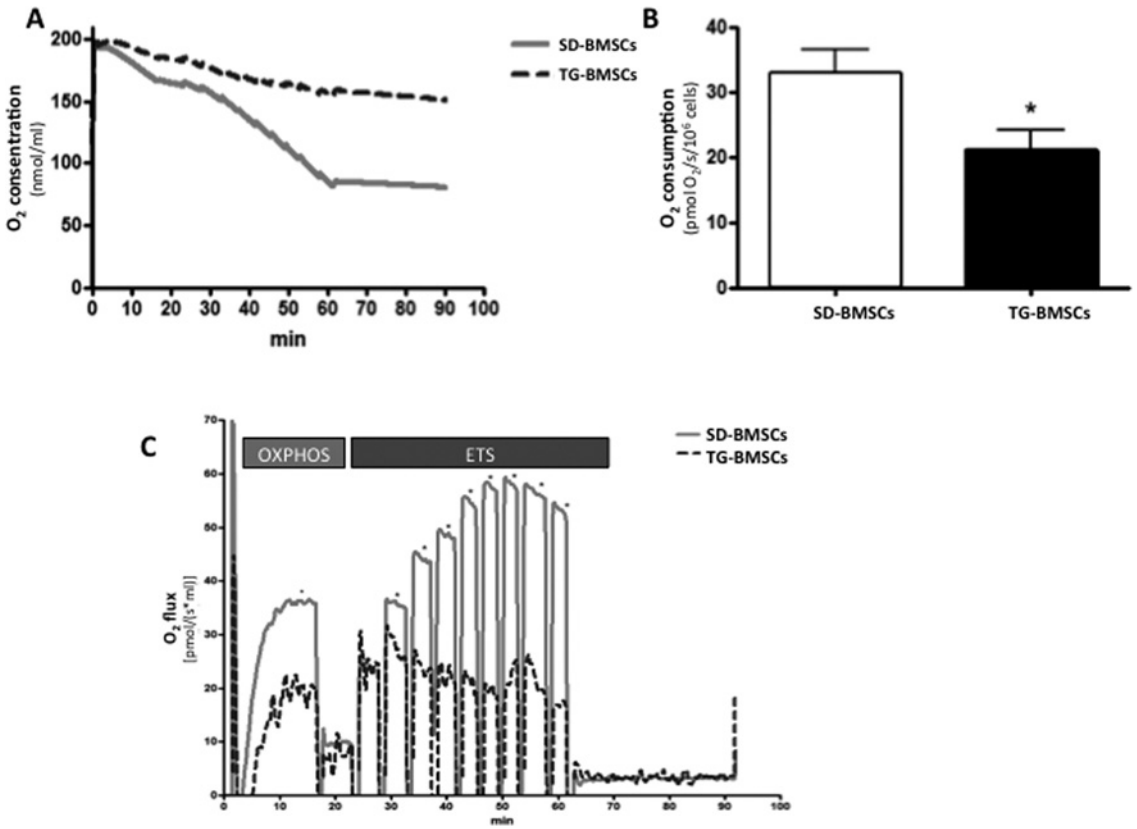

Figure 6 **High-resolution respirometry of SD- and TG-BMSCs**
(**A**) Oxygen (O_2) use over time, (**B**) quantification of basal oxygen consumption, and (**C**) evaluation of oxidative phosphorylation (OXPHOS) and functionality of the electron transport chain (ETS) in SD- and TG-BMSCs. $^*P < 0.05$ between plateaus (SD- compared with TG-BMSCs).

Table 1 **List of KEGG pathways associated with genes up-regulated in the dTGR BMSCs vs control cells as found by microarrays to KEGG pathways**

KEGG pathway	Number of genes	p-value	List of genes associated with KEGG-pathways, downregulated marked with light blue, upregulated with orange color.														
Chemokine signaling pathway	15	1.1E-4	Ptk2	Cxcl10	Gng13	Pf4	Ccl1	Ccl2	Ccl20	Ccl7	Cxcl1	Cxcl12	Cxcl13	Cxcl16	Cxcl2	Cx3cl1	Nfkbia
Cytokine-cytokine receptor interaction	15	5.0E-4	Cxcl10	Pf4	Tnfrsf11b	Il23a	Ccl2	Cxcl12	Cxcl13	Cxcl16	Cxcl2	Cx3cl1	Csf2	Csf3	Il1a	Il1r2	Il6
Prion diseases	6	1.8E-3	Casp12	C1qa	C1qb	Ncam1	Il1a	Il6									
Toll-like receptor signaling pathway	9	2.1E-3	Cxcl10	Irf7	Spp1	Tlr6	Il6	Lbp	Map3k8	Nfkbia	Tlr2						
Hematopoietic cell lineage	8	3.7E-3	RT1-Da	Itga1	Cd55	Csf2	Csf3	Il1a	Il1r2	Il6							
ECM-receptor interaction	8	4.6E-3	Col3a1	Col11a1	Itga1	Itga11	Spp1	Sdc2	Thbs4	Thbs2							
Vascular smooth muscle contraction	9	8.4E-3	Actg2	Itpr1	Myh11	Ppp1r14a	Ramp1	Adora2b	Agtr1a	Pla2g2a	Ramp3						
Complement and coagulation cascades	7	8.9E-3	C1qa	C1qb	Cd55	Bdkrb1	C3	Serping1	C1s								
Pathways in cancer	16	1.6E-2	Ptk2	Cdkn2a	Fzd8	Pparg	Egln3	Epas1	Il6	Mmp2	Mmp9	Nfkbia	Pax8	Ptgs2	Nos2	_OC687813	Slc2a1	Wnt5a
NOD-like receptor signaling pathway	6	2.1E-2	Ccl2	Ccl7	Cxcl1	Cxcl2	Il6	Nfkbia									
Focal adhesion	11	2.8E-2	Ptk2	Cav3	Col3a1	Col11a1	Ccnd2	Itga1	Itga11	Spp1	Thbs4	Vcl	Thbs2				
PPAR signaling pathway	6	3.5E-2	Apoc3	Olr1	Pparg	Angptl4	Fads2	Lpl									
Viral myocarditis	6	7.3E-2	RT1-Da	Myh11	Myh8	Myh1	Cd55	RT1-CE2									
Leukocyte transendothelial migration	7	7.5E-2	Ptk2	Vcl	Nox1	Cxcl12	Cldn3	Mmp2	Mmp9								
Calcium signaling pathway	9	9.7E-2	Atp2a1	Itpr1	Pln	Tbxa2r	Adora2b	Agtr1a	Bdkrb1	Ednrb	Nos2						

in pathological compromise of BMSCs' therapeutic functions. This was associated with an inflammatory phenotype that persisted even under cell culture conditions when cells were expanded for therapy devoid of their environmental systemic or niche stimuli. In the dTGR animals, the expression of transgenes occurs throughout the lifespan of the animals. Thus elevated levels of AngII affect and guide, both directly and indirectly, cell differentiation in the bone marrow from very early on. Such a tenacious effect may be able to completely reprogramme the haemopoietic niche environment. Upon cell harvesting from bone marrow, this in turn would manifest as isolation of an altered phenotype of BMSCs, as seen in the present study. Our results warrant further investigation into the direct and indirect roles of AngII on the dTGR bone marrow and its microenvironment for elucidation of cell type composition and functional changes during disease progression.

Exacerbation of AKI by administration of TG-BMSCs can be attributable to a direct effect via the cells' production of angiotensinogen or a pronounced pro-inflammatory mediator secretion promoted by the TG-BMSCs' pro-inflammatory phenotype. The relative discrepancy of reduced macrophage activation (ED-1 immunoreactivity) and kidney MCP-1 expression by both

Table 2 Genes involved in RAS
n.s., not significant.

Probe	Gene	Symbol	mRNA RefSEQ	SD-BMSC normalized expression	TG-BMSC normalized expression	Fold change	
A_64_P098230	Angiotensin I-converting enzyme (peptidyl-dipeptidase A) 1	Ace	NM_012544	6.51	6.445	−0.1	n.s.
A_64_P132696	Angiotensin I-converting enzyme (peptidyl-dipeptidase A) 2	Ace2	NM_001012006	6.01	6.02	0.0	n.s.
A_64_P154849	Angiotensinogen (serpin peptidase inhibitor, clade A, member 8)	Agt	NM_134432	6.01	6.25	0.2	n.s.
A_42_P486203	**Angiotensin II receptor, type 1a**	**Agtr1a**	**NM_030985**	**6.27**	**9.08**	**2.8**	**Up-regulated**
A_64_P109894	Angiotensin II receptor, type 1b	Agtr1b	NM_031009	6.04	6	0.0	n.s.
A_64_P097458	Angiotensin II receptor, type 2	Agtr2	NM_012494	6	6	0.0	n.s.
A_44_P500013	Alanyl (membrane) aminopeptidase	Anpep	NM_031012	8.71	8.19	−0.5	n.s.
A_44_P1029706	Chymase 1, mast cell	Cma1	NM_013092	6.06	6.11	0.1	n.s.
A_43_P15942	Carboxypeptidase A3, mast cell	Cpa3	NM_019300	6.44	6.33	−0.1	n.s.
A_44_P474755	Cathepsin A	Ctsa	NM_001011959	16.62	16.72	0.1	n.s.
A_64_P106673	Cathepsin G	Ctsg	NM_001106041	6.05	6.04	0.0	n.s.
A_44_P209788	**Glutamyl aminopeptidase**	**Enpep**	**NM_022251**	**9.54**	**11.28**	**1.7**	**Up-regulated**
A_64_P337849	Leucyl/cystinyl aminopeptidase	Lnpep	NM_133574	9.34	9.32	0.0	n.s.
A_44_P1029253	MAS1 oncogene	Mas1	NM_012757	6.08	6.12	0.0	n.s.
A_44_P530801	Mast cell protease 8-like 2	Mcpt8l2	NM_001135010	5.98	5.99	0.0	n.s.
A_44_P204710	Mast cell protease 8-like 3	Mcpt8l3	NSRNOT0000004931	6.25	6.26	0.0	n.s.
A_43_P11484	**Membrane metallo-endopeptidase**	**Mme**	**NM_012608**	**8.5**	**7.38**	**−1.1**	**Down-regulated**
A_44_P271643	Neurolysin (metallopeptidase M3 family)	Nln	NM_053970	8.62	8.54	−0.1	n.s.
A_64_P059056	Renin	Ren	NM_012642	12.89	12.16	−0.7	n.s.
A_44_P412092	Thimet oligopeptidase 1	Thop1	NM_172075	12.56	12.43	−0.1	n.s.

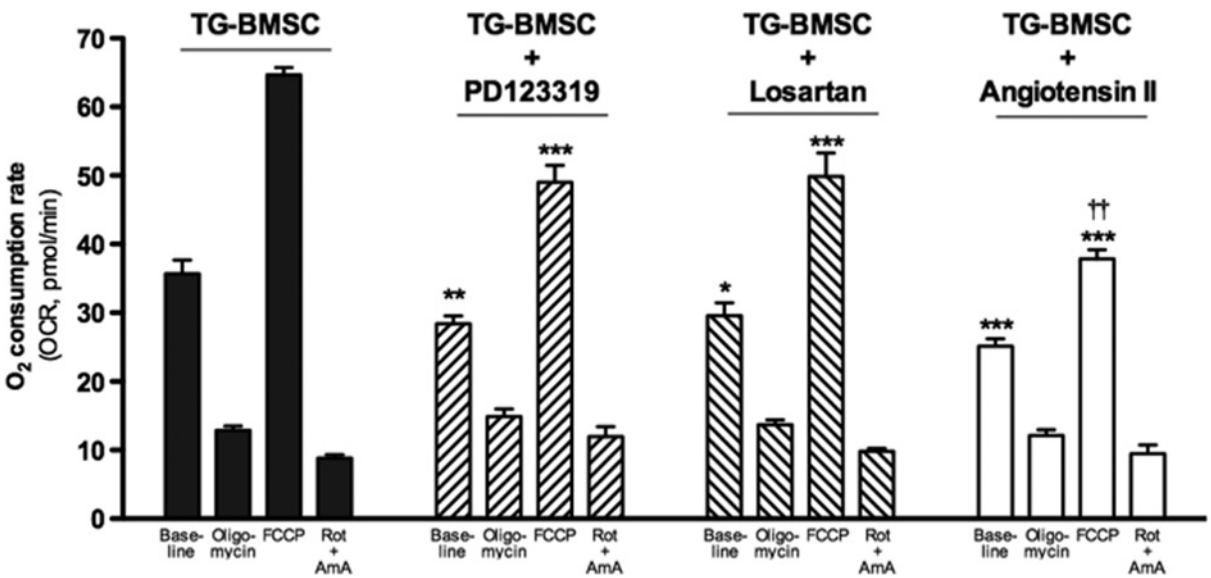

Figure 7 Mitochondrial respiration in TG-BMSCs
Analysis of blockade of AT_1 (losartan, 10 μM) or AT_2 (PD123319, 10 μM) receptors as well as stimulation with exogenous AngII (100 nM) on mitochondrial oxygen consumption in TG-BMSCs. $^{**}P < 0.01$, $^{***}P < 0.001$ as compared with the respective measurement in untreated TG-BMSCs. $\dagger\dagger P < 0.01$ between AngII and both PD123319 and losartan-treated groups. AmA, antimycin A; Rot, rotenone.

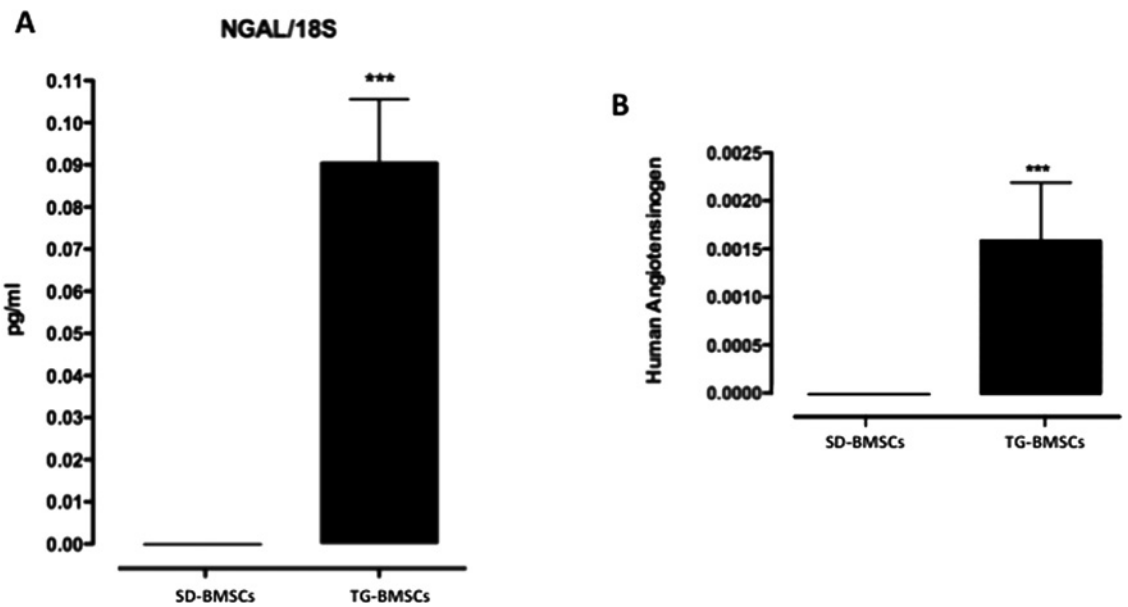

Figure 8 Expression of NGAL and the human angiotensinogen transgene in BMSCs
Evaluation of (**A**) lipocalin 2 (NGAL) and (**B**) human angiotensinogen transgene in SD- and TG-BMSCs. $^{***}P < 0.001$ between cell types.

SD- and TG-BMSCs can be due to the anti-inflammatory activity of SD cells and on the other hand to aggravation of tissue injury by TG-BMSCs. Dramatic deterioration of kidney function was evident by increased mortality after administering the higher dose (6×10^6) of TG-BMSCs. Increased tissue damage could alter and speed up inflammation kinetics [34], that, at the end of the 48-h follow-up in the aftermath of the inflammatory insult, manifests as already reduced expression of inflammatory injury markers. It can also be speculated that not all cells injected into the descending aorta reach the kidneys, but infiltrate other organs instead. The contribution of different tissue distribution of TG-BMSCs, such as accumulation in the lungs and a subsequent pulse in systemic AngII production and hypertensive crisis, cannot be ruled out as a possible cause of their lethal actions.

AT_1 receptor signalling has been tightly linked with inflammation [35]. In the present study we found increased

expression of AT_1 in TG-BMSCs associated with a highly proliferative pro-inflammatory phenotype. The contribution of autocrine AT_1 stimulation by AngII generated by cultured TG-BMSCs on their inflammatory phenotype requires further investigation. We showed in the present study that inhibition of AT_1 or AT_2 signalling leads to inhibition of mitochondrial respiration, and that exogenously added AngII also potently causes inhibition of mitochondrial function in TG-BMSCs. This result suggests that AngII signalling in these cells utilizes both receptor subtypes and that there may exist inhibitory cross-talk between the receptors or in downstream signalling from these receptors. When this cross-talk is inhibited by blockade of either receptor subtype, signalling by the other type to inhibit mitochondrial respiration is augmented. The fact that exogenous AngII was effective in reducing mitochondrial respiration further suggests that the AngII signalling pathway is active in the TG-BMSCs, and indeed acts to inhibit basal as well as stimulated mitochondrial respiration. Our results, however, showed that TG-BMSCs do not express the human renin transgene suggesting alternative mechanism(s) of AngII generation from the expressed human angiotensinogen to stimulate AT_1 receptors or a receptor-independent effect. In fact, at least AngII has been shown to increase proliferation independently of the AT_1 receptor [36]. On the other hand, Crowley et al. [37] have reported a protective role for AT_1 receptor on bone-marrow-derived cells in chronic hypertension. They also found that animals with bone marrow AT_1 receptor expression knocked out responded to hypertension with increased renal accumulation of mononuclear cells. Taken together with our results on suppression of ED-1 and MCP-1 levels, it is tempting to say that our results indicate (via an as-yet-unknown mechanism) an AT_1 expression-dependent anti-chemotactic or anti-inflammatory effect of BMSCs on monocytes.

Although it has been postulated that rat renin only cleaves rat angiotensinogen, it is also possible that rat enzymes (renin, angiotensin-converting enzyme, MMPs, cathepsins etc.) as produced and/or induced in the TG-BMSCs may be able to cleave a fraction of the human angiotensinogen to angiotensin I and then to AngII. AngII could also be formed independently of renin via Ang(1–12)-utilizing enzymatic pathways not yet fully characterized, but putatively involving chymase, cathepsins or components of the kallikrein/kinin system [38]. Interestingly, a redox modification of angiotensinogen structure was previously identified to contribute to the predisposition of angiotensinogen to cleavage by renin [39]. The observed increased ROS production in the TG-BMSCs could thus in fact contribute to modulation of cleavage of the overtly produced angiotensinogen, and possibly modify the TG-BMSC-produced angiotensinogen in such a manner that it becomes more readily accessible to cleavage. Bone marrow cells have been shown to respond to AngII by increased proliferation [40], and the BM-RAS has been tightly linked to control of cell maturation and haemopoiesis [5]. This was also indicated in our gene expression screening by the differential regulation of the KEGG haemopoietic cell lineage pathway. Our results also suggested a differential mitochondrial regulation to increased age in cell culture between SD- and TG-BMSCs. Furthermore, since an inflammatory phenotype, ROS and dysfunctional mitochondria are associated with senescence signalling in culture [41], it is feasible that pathological RAS-related changes may impede normal regulation of pathways related to cell differentiation and senescence. The contribution of autocrine effects of AngII on the TG-BMSC phenotype and the extent as well as the mechanism of angiotensinogen cleavage given the apparent lack of renin expression by these cells warrant further studies.

Indications from the microarrays suggest that the TG-BMSC phenotype is massively affected on gene expression level by factors that guide cell adherence (decorin, lumican, etc.), inflammatory phenotype and proliferation (cytokines, chemokines), reactive oxygen radical production [NOX1/dual oxidase 1 (DUOX1)] and protection against injury [NGAL (lipocalin 2), superoxide dismutase (SOD)]. In *lcn2*$^{-/-}$ murine embryonic fibroblasts (MEFs), lipocalin 2 deficiency has been associated with a reduction in peroxisome-proliferator-activated receptor γ coactivator 1α (PGC1α) expression and further linked to decreased cell proliferation, autophagy and mitochondrial biogenesis [42]. Taken together with our data, an increase in lipocalin 2 may, in turn, positively modulate these mitochondrial effects. Furthermore, lipocalin 2 has been shown to protect cells against oxidative stress [43]. In our data, SOD2 (mitochondrial SOD, maganese-SOD) as a marker of oxidative stress response was 22-fold upregulated in TG-BMSCs as compared with SD-BMSCs.

Lipocalin 2 was initially identified as being in a complex with MMP-9 [44]. It protects the protease from degradation and sustains its proteolytic activity. Thus the immense combined induction of both lipocalin 2 and MMP-9, as we observed in the microarrays, suggests increased proteolytic activity in the TG-BMSCs. In keeping with the pro-inflammatory activation of TG-BMSCs, as shown by increased expression of several cytokines and chemokines in our data, lipocalin 2 induction is driven by NF-κB (nuclear factor κB) activation via cytokines such as interleukin 1 (IL-1), and it has been shown to stimulate neutrophil chemotaxis [45]. As lipocalin 2 is rapidly induced in the kidney after injury, it is considered an early biomarker and a predictor of poor outcome in AKI [46]. The immensely induced expression of lipocalin 2 in TG-BMSCs could thus either directly or indirectly contribute to the exacerbation of AKI in our model. Interestingly, also decorin (*dcn*), found to be increased in TG-BMSCs (Supplementary Table SI), has been implicated in enhancing inflammatory responses [47] through inhibition of anti-inflammatory transforming growth factor-β (TGF-β)-mediated signalling. In contrast, because the alarm antiprotease secretory leucocyte protease inhibitor (SLPI) has been shown to inhibit proteolytic activity [48], it can be argued that its induced expression in TG-BMSCs may serve as an autoprotective act to counterbalance the proteolytic and pro-inflammatory gene expression in TG cells. Expression of SLPI was induced more than 2200-fold in TG-BMSCs (Supplementary Table SI).

Taken together, these data imply that TG-BMSCs may promote the acute inflammatory response in AKI. The cells' inflammatory phenotype may be a result of irreversible bone marrow changes. Moreover, the expression of genes associated with modulation and suppression of TGF-β signalling may further aggravate the inflammatory condition [49]. Our data also suggest that the cellular response to the specific modifications of RAS in

dTGR is counteracted, at least to some extent, by an autoprotective response as shown by increased ROS formation counteracted by induction of anti-oxidative lipocalin 2 and MnSOD or by increased expression of MMPs counteracted by induction of SLPI.

In conclusion, modification of BM-RAS may convey unprecedented dramatic effects via the release and tissue infiltration of BMSCs as a normal inherent reactivity to injury. Our data provide the first evidence of high angiotensinogen production in BMSCs inducing an AngII-like cellular response in an intracrine or autocrine manner, and subsequent dramatic deterioration of the BMSCs' regenerative responses. Our data address the urgent need for further studies to specifically address the mechanisms of BM-RAS components guiding the therapeutic effects of BMSCs.

CLINICAL PERSPECTIVES

- Hypertension and persistent activation of the renin–angiotensin system (RAS) can predispose to acute kidney injury (AKI).
- We investigated the effect of RAS activation on the therapeutic action of bone-marrow-derived stromal cells (BMSCs) in a rat model of AKI.
- Our results demonstrate that persistent RAS activation induces an inflammatory BMSC phenotype and dramatically compromises the tissue-repair functions of BMSCs. Dysfunctional BMSCs in hypertension may exacerbate associated end-organ disease.

AUTHOR CONTRIBUTION

Esko Kankuri and Eero Mervaala designed and supervised the work, analysed the data, and co-wrote the paper. Elina Mervaala, Piet Finckenberg and Aija Ahola conducted the studies and analysed the data. Markus Storvik performed data analysis and bioinformatics. Jouko Levijoki provided critical reagents and clinical chemistry analyses services. Dominik Müller provided critical experimental animals and reagents.

ACKNOWLEDGEMENTS

We thank Nada Bechara-Hirvonen and Päivi Leinikka for their skilful technical assistance.

FUNDING

This work was supported by the Sigrid Jusélius Foundation, the Finnish Foundation for Cardiovascular Research and the Academy of Finland (275882).

REFERENCES

1 Luft, F.C., Mervaala, E., Muller, D.N., Gross, V., Schmidt, F., Park, J.K., Schmitz, C., Lippoldt, A., Breu, V., Dechend, R. et al. (1999) Hypertension-induced end-organ damage: a new transgenic approach to an old problem. Hypertension **33**, 212–218 CrossRef PubMed

2 Volpe, M., Savoia, C., De Paolis, P., Ostrowska, B., Tarasi, D. and Rubattu, S. (2002) The renin-angiotensin system as a risk factor and therapeutic target for cardiovascular and renal disease. J. Am. Soc. Nephrol. **13** (Suppl. 3), S173–S178 CrossRef PubMed

3 Bader, M. (2010) Tissue renin-angiotensin-aldosterone systems: targets for pharmacological therapy. Annu. Rev. Pharmacol. Toxicol. **50**, 439–465 CrossRef PubMed

4 Strawn, W.B., Richmond, R.S., Ann Tallant, E., Gallagher, P.E. and Ferrario, C.M. (2004) Renin-angiotensin system expression in rat bone marrow haematopoietic and stromal cells. Br. J. Haematol. **126**, 120–126 CrossRef PubMed

5 Durik, M., Sevá Pessôa, B. and Roks, A.J.M. (2012) The renin-angiotensin system, bone marrow and progenitor cells. Clin. Sci. **123**, 205–223 CrossRef PubMed

6 Sinka, L., Biasch, K., Khazaal, I., Péault, B. and Tavian, M. (2012) Angiotensin-converting enzyme (CD143) specifies emerging lympho-hematopoietic progenitors in the human embryo. Blood **119**, 3712–3723 CrossRef PubMed

7 Numasawa, Y., Kimura, T., Miyoshi, S., Nishiyama, N., Hida, N., Tsuji, H., Tsuruta, H., Segawa, K., Ogawa, S. and Umezawa, A. (2011) Treatment of human mesenchymal stem cells with angiotensin receptor blocker improved efficiency of cardiomyogenic transdifferentiation and improved cardiac function via angiogenesis. Stem Cells **29**, 1405–1414 PubMed

8 Beyazit, Y., Purnak, T., Guven, G.S. and Haznedaroglu, I.C. (2010) Local bone marrow renin-angiotensin system and atherosclerosis. Cardiol. Res. Pract. **2011**, 714515 PubMed

9 Haznedaroglu, I.C. and Beyazit, Y. (2010) Pathobiological aspects of the local bone marrow renin-angiotensin system: a review. J. Renin Angiotensin Aldosterone Syst. **11**, 205–213 CrossRef PubMed

10 Bonventre, J.V. and Yang, L. (2011) Cellular pathophysiology of ischemic acute kidney injury. J. Clin. Invest. **121**, 4210–4221 CrossRef PubMed

11 Sharfuddin, A.A. and Molitoris, B.A. (2011) Pathophysiology of ischemic acute kidney injury. Nat. Rev. Nephrol. **7**, 189–200 CrossRef PubMed

12 Acute Kidney Injury Work Group (2012) KDIGO Clinical Practice Guideline for Acute Kidney Injury. Kidney Int. Suppl. **2**, 1–138 CrossRef

13 Humphreys, B.D. and Bonventre, J.V. (2008) Mesenchymal stem cells in acute kidney injury. Annu. Rev. Med. **59**, 311–325 CrossRef PubMed

14 Tögel, F.E. and Westenfelder, C. (2010) Mesenchymal stem cells: a new therapeutic tool for AKI. Nat. Rev. Nephrol. **6**, 179–183 CrossRef PubMed

15 Burger, D., Gutsol, A., Carter, A., Allan, D.S., Touyz, R.M. and Burns, K.D. (2012) Human cord blood CD133+ cells exacerbate ischemic acute kidney injury in mice. Nephrol. Dial. Transplant **27**, 3781–3789 CrossRef PubMed

16 Mervaala, E., Muller, D.N., Schmidt, F., Park, J.K., Gross, V., Bader, M., Breu, V., Ganten, D., Haller, H. and Luft, F.C. (2000) Blood pressure-independent effects in rats with human renin and angiotensinogen genes. Hypertension **35**, 587–594 CrossRef PubMed

17 St-Jacques, R., Toulmond, S., Auger, A., Binkert, C., Cromlish, W., Fischli, W., Harris, J., Hess, P., Lan, J., Liu, S. et al. (2011) Characterization of a stable, hypertensive rat model suitable for the consecutive evaluation of human renin inhibitors. J. Renin Angiotensin Aldosterone Syst. **12**, 133–145 CrossRef PubMed

18 Bohlender, J., Fukamizu, A., Lippoldt, A., Nomura, T., Dietz, R., Ménard, J., Murakami, K., Luft, F.C. and Ganten, D. (1997) High human renin hypertension in transgenic rats. Hypertension **29**, 428–434 CrossRef PubMed

19 Mervaala, E.M., Müller, D.N., Park, J.K., Schmidt, F., Löhn, M., Breu, V., Dragun, D., Ganten, D., Haller, H. and Luft, F.C. (1999) Monocyte infiltration and adhesion molecules in a rat model of high human renin hypertension. Hypertension **33**, 389–395 CrossRef PubMed

20 Ganten, D., Wagner, J., Zeh, K., Bader, M., Michel, J.B., Paul, M., Zimmermann, F., Ruf, P., Hilgenfeldt, U., Ganten, U. et al. (1992) Species specificity of renin kinetics in transgenic rats harboring the human renin and angiotensinogen genes. Proc. Natl. Acad. Sci. U.S.A. **89**, 7806–7810 CrossRef PubMed

21 Kaergel, E., Muller, D.N., Honeck, H., Theuer, J., Shagdarsuren, E., Mullally, A., Luft, F.C. and Schunck, W.-F. (2002) P450-dependent arachidonic acid metabolism and angiotensin II-induced renal damage. Hypertension **40**, 273–279 CrossRef PubMed

22 den Hollander, B., Sundström, M., Pelander, A., Ojanperä, I., Mervaala, E., Korpi, E.R. and Kankuri, E. (2014) Keto amphetamine toxicity-focus on the redox reactivity of the cathinone designer drug mephedrone. Toxicol. Sci. **141**, 120–131 CrossRef PubMed

23 Kennedy, S.E. and Erlich, J.H. (2008) Murine renal ischaemia-reperfusion injury. Nephrology **13**, 390–396 CrossRef PubMed

24 Lempiäinen, J., Finckenberg, P., Levijoki, J. and Mervaala, E. (2012) AMPK activator AICAR ameliorates ischaemia reperfusion injury in the rat kidney. Br. J. Pharmacol. **166**, 1905–1915 CrossRef PubMed

25 Devarajan, P. (2010) Neutrophil gelatinase-associated lipocalin: a promising biomarker for human acute kidney injury. Biomark. Med. **4**, 265–280 CrossRef PubMed

26 Huo, W., Zhang, K., Nie, Z., Li, Q. and Jin, F. (2010) Kidney injury molecule-1 (KIM-1): a novel kidney-specific injury molecule playing potential double-edged functions in kidney injury. Transplant. Rev. (Orlando) **24**, 143–146 CrossRef PubMed

27 Finckenberg, P., Eriksson, O., Baumann, M., Merasto, S., Lalowski, M.M., Levijoki, J., Haasio, K., Kytö, V., Muller, D.N., Luft, F.C. et al. (2012) Caloric restriction ameliorates angiotensin II-induced mitochondrial remodeling and cardiac hypertrophy. Hypertension **59**, 76–84 CrossRef PubMed

28 Balaban, R.S., Nemoto, S. and Finkel, T. (2005) Mitochondria, oxidants, and aging. Cell **120**, 483–495 CrossRef PubMed

29 Chance, B., Sies, H. and Boveris, A. (1979) Hydroperoxide metabolism in mammalian organs. Physiol. Rev. **59**, 527–605 PubMed

30 Bulua, A.C., Simon, A., Maddipati, R., Pelletier, M., Park, H., Kim, K.-Y., Sack, M.N., Kastner, D.L. and Siegel, R.M. (2011) Mitochondrial reactive oxygen species promote production of proinflammatory cytokines and are elevated in TNFR1-associated periodic syndrome (TRAPS). J. Exp. Med. **208**, 519–533 CrossRef PubMed

31 Finkel, T. (2011) Signal transduction by reactive oxygen species. J. Cell Biol. **194**, 7–15 CrossRef PubMed

32 Jun, J.Y., Zubcevic, J., Qi, Y., Afzal, A., Carvajal, J.M., Thinschmidt, J.S., Grant, M.B., Mocco, J. and Raizada, M.K. (2012) Brain-mediated dysregulation of the bone marrow activity in angiotensin II-induced hypertension. Hypertension **60**, 1316–1323 CrossRef PubMed

33 Zubcevic, J., Santisteban, M.M., Pitts, T., Baekey, D.M., Perez, P.D., Bolser, D.C., Febo, M. and Raizada, M.K. (2014) Functional neural-bone marrow pathways: implications in hypertension and cardiovascular disease. Hypertension **63**, e129–e139 CrossRef PubMed

34 Jang, H.R. and Rabb, H. (2015) Immune cells in experimental acute kidney injury. Nat. Rev. Nephrol. **11**, 88–101 CrossRef PubMed

35 Benigni, A., Cassis, P. and Remuzzi, G. (2010) Angiotensin II revisited: new roles in inflammation, immunology and aging. EMBO Mol. Med. **2**, 247–257 CrossRef PubMed

36 Baker, K.M. and Kumar, R. (2006) Intracellular angiotensin II induces cell proliferation independent of AT1 receptor. Am. J. Physiol. Cell Physiol. **291**, C995–C1001 CrossRef PubMed

37 Crowley, S.D., Song, Y.-S., Sprung, G., Griffiths, R., Sparks, M., Yan, M., Burchette, J.L., Howell, D.N., Lin, E.E. and Okeiyi, B. (2010) A role for angiotensin II type 1 receptors on bone marrow-derived cells in the pathogenesis of angiotensin II-dependent hypertension. Hypertension **55**, 99–108 CrossRef PubMed

38 Carey, R.M. (2013) Newly discovered components and actions of the renin-angiotensin system. Hypertension **62**, 818–822 CrossRef PubMed

39 Zhou, A., Carrell, R.W., Murphy, M.P., Wei, Z., Yan, Y., Stanley, P.L.D., Stein, P.E., Broughton Pipkin, F. and Read, R.J. (2010) A redox switch in angiotensinogen modulates angiotensin release. Nature **468**, 108–111 CrossRef PubMed

40 Rodgers, K.E., Xiong, S., Steer, R. and diZerega, G.S. (2000) Effect of angiotensin II on hematopoietic progenitor cell proliferation. Stem Cells **18**, 287–294 CrossRef PubMed

41 Kuilman, T., Michaloglou, C., Mooi, W.J. and Peeper, D.S. (2010) The essence of senescence. Genes Dev. **24**, 2463–2479 CrossRef PubMed

42 Jin, D., Zhang, Y. and Chen, X. (2011) Lipocalin 2 deficiency inhibits cell proliferation, autophagy, and mitochondrial biogenesis in mouse embryonic cells. Mol. Cell. Biochem. **351**, 165–172 CrossRef PubMed

43 Roudkenar, M.H., Halabian, R., Bahmani, P., Roushandeh, A.M., Kuwahara, Y. and Fukumoto, M. (2011) Neutrophil gelatinase-associated lipocalin: a new antioxidant that exerts its cytoprotective effect independent on heme oxygenase-1. Free Radic. Res. **45**, 810–819 CrossRef PubMed

44 Yan, L., Borregaard, N., Kjeldsen, L. and Moses, M.A. (2001) The high molecular weight urinary matrix metalloproteinase (MMP) activity is a complex of gelatinase B/MMP-9 and neutrophil gelatinase-associated lipocalin (NGAL). Modulation of MMP-9 activity by NGAL. J. Biol. Chem. **276**, 37258–37265 PubMed

45 Chakraborty, S., Kaur, S., Guha, S. and Batra, S.K. (2012) The multifaceted roles of neutrophil gelatinase associated lipocalin (NGAL) in inflammation and cancer. Biochim. Biophys. Acta. **1826**, 129–169 PubMed

46 Haase, M., Devarajan, P., Haase-Fielitz, A., Bellomo, R., Cruz, D.N., Wagener, G., Krawczeski, C.D., Koyner, J.L., Murray, P. and Zappitelli, M. (2011) The outcome of neutrophil gelatinase-associated lipocalin-positive subclinical acute kidney injury: a multicenter pooled analysis of prospective studies. J. Am. Coll. Cardiol. **57**, 1752–1761 CrossRef PubMed

47 Merline, R., Moreth, K., Beckmann, J., Nastase, M.V., Zeng-Brouwers, J., Tralhão, J.G., Lemarchand, P., Pfeilschifter, J., Shaefer, R.M., Iozzo, R.V., Schaefer, L. et al. (2011) Signaling by the matrix proteoglycan decorin controls inflammation and cancer through PDCD4 and microRNA-21. Sci. Signal. **4**, ra75 PubMed

48 Williams, S.E., Brown, T.I., Roghanian, A. and Sallenave, J.-M. (2006) SLPI and elafin: one glove, many fingers. Clin. Sci. **110**, 21–35 CrossRef PubMed

49 Gentle, M.E., Shi, S., Daehn, I., Zhang, T., Qi, H., Yu, L., D'Agati, V.D., Schlondorff, D.O. and Bottinger, E.P. (2013) Epithelial cell TGFβ signaling induces acute tubular injury and interstitial inflammation. J. Am. Soc. Nephrol. **24**, 787–799 CrossRef PubMed

Received 22 July 2014/15 December 2014; accepted 23 December 2014

Published as Immediate Publication 23 December 2014, doi: 10.1042/CS20140445